



Preparation and Study on Nitrogen- and Phosphorus- Containing Fire Resistant Coatings for Wood by UV-Cured Methods

Guoru Ma^{1,2}, Xuan Wang³, Wei Cai¹, Chao Ma¹, Xin Wang¹, Yulu Zhu¹, Yongchun Kan¹, Weiyi Xing^{1*} and Yuan Hu^{1,3*}

¹State Key Laboratory of Fire Science, University of Science and Technology of China, Hefei, China, ²Beijing Building Materials Testing Academy Co., Ltd., National Center for Safety Quality Supervision and Testing of Fire-proof Building Products, Beijing, China, ³Nano Science and Technology Institute, University of Science and Technology of China, Suzhou, China

OPEN ACCESS

Edited by:

Wei Wu,
City University of Hong Kong, Hong
Kong, SAR China

Reviewed by:

Dong Wang,
Jiangnan University, China
Gang Tang,
Anhui University of Technology, China
Yao Yuan,
Xiamen University of Technology,
China

*Correspondence:

Weiyi Xing
xingwy@ustc.edu.cn
Yuan Hu
yuanhu@ustc.edu.cn

Specialty section:

This article was submitted to
Polymeric and Composite Materials,
a section of the journal
Frontiers in Materials

Received: 10 January 2022

Accepted: 18 January 2022

Published: 04 March 2022

Citation:

Ma G, Wang X, Cai W, Ma C, Wang X,
Zhu Y, Kan Y, Xing W and Hu Y (2022)
Preparation and Study on Nitrogen-
and Phosphorus- Containing Fire
Resistant Coatings for Wood by UV-
Cured Methods.
Front. Mater. 9:851754.
doi: 10.3389/fmats.2022.851754

Wood has been widely used since ancient times due to its biodegradability, good elasticity, impact resistance, and easy availability. However, the flammability of wood has vastly limited its applications and the fire hazard of wood has cost a great loss of life and property. Thus, it is important to improve the fire resistance of wood. Here, we used a phosphate acrylate monomer (PGMA) which was synthesized with phosphoric acid and glycidyl methacrylate by ring-opening reaction and melamine acrylic ester (MAAR) to make up a series of fireproof coatings with different proportions, and the fire resistance of wood has been investigated using the limiting oxygen index (LOI) test, back temperature test, and cone calorimeter test. When the wood was coated with the composite of 33.3% PGMA and 66.7% MAAR, the total heat release value decreased from 39.0 to 38.2 MJ/m², and the total smoke release value decreased from 622 to 512 m²/m², showing a remarkable improvement in fire resistance and smoke suppression. Thus, this easily prepared, cheap, and effective flame retardant coating can promote a wider application of wood.

Keywords: wood, synergistic effect, UV-cured, fire resistance, coatings

1 INTRODUCTION

Wood has had a wide application in construction, furniture, and decoration since ancient times, due to its biodegradability, good elasticity, impact resistance, and malleability. However, the inflammability of wood results in many fire hazards, which seriously restricts its application (Ma et al., 2019; Ma et al., 2020). Therefore, it is important to improve the flame resistance of wood by several methods to extend its use. Usually, impregnation and surface coating are the main strategies to reduce the flammability of wood (Guo et al., 2017; Song et al., 2020). Impregnation means impregnating the flame retardants into the porous structure of wood with a vacuum-pressure technique (Lu et al., 2021). The naturally porous structure of wood can provide access for flame retardants. For example, the limiting oxygen index (LOI) value has been increased from 23 to 78% after being impregnated with a 25% solution of nitrogen-phosphorous-based flame retardant which is coupled with reactive formaldehyde (UF) oligomer (Jiang et al., 2015). Pabeliña et al. (2012) investigated the effects of chemical and

plasma treatment on the flame retardancy of wood samples by impregnation. However, the mechanical properties of wood would be destroyed after impregnation.

Compared with impregnation, surface coating is an effective way to improve the fire resistance of wood with less destruction in mechanical properties. Halogen-free flame retardants are widely used in coatings, because of less release of pollution and toxic gases during combustion, especially for phosphorus- and nitrogen-containing flame retardants (Yan et al., 2018; Yan et al., 2019). For example, acrylate oligomers were blended with phosphorus, nitrogen, and sulfur monomers to fabricate flame retardant coatings, while the results revealed a better fire resistance of wood when the proportion of phosphorus and nitrogen monomers was 2:4 (Wang et al., 2018). Previous work utilized Mg-Al LDH to fabricate flame retardant coatings of wood, which improved the LOI value to 39.1% from 18.9%, suggesting an excellent fire resistance of coated wood (Guo et al., 2017). Therefore, surface coating composed of phosphorus- and nitrogen-containing flame retardants is a beneficial to improve the fire resistance of wood.

UV curing is a kind of photochemistry, featuring an efficient and fast way to transform a low molecular material into a cross-linked polymer (Yan et al., 2017; Xu et al., 2018). In general, the photoinitiator in the liquid UV materials is stimulated to produce radicals or cations under UV light, thereby initiating the polymerization of precursors containing active functional groups (Han et al., 2007; Xu et al., 2018). The UV-curing method has the advantage of immediate drying and purifying which enables its wide applications in the coatings. For example, a mussel-inspired transparent intumescent flame retardant bio-coating for wood products was cured under the irradiation of ultraviolet light. Furthermore, the UV-curing method leads to less destruction of the mechanical properties of the wood (Ma et al., 2020). However, the reports of highly efficient flame retardant coatings fabricated by UV-cured technology towards wood are still very few.

In this work, a novel, easy-prepared, and transparent fire resistance coating for wood was fabricated by UV curing. A phosphate acrylate monomer (PGMA) was synthesized with the ring-opening reaction between phosphoric acid and glycidyl methacrylate. Then, PGMA was incorporated with melamine acrylic ester (MAAR) to fabricate a series of fireproof coatings of wood at different ratios. The fire resistance of coated wood was scrupulously investigated with back temperature, limiting oxygen index, and cone calorimeter tests.

2 EXPERIMENTAL

A schematic diagram of fabricating coated wood was shown in **Figure 1**.

2.1 Materials

Phosphorus acid was supplied by Aladdin brand, glycidyl methacrylate (GMA) was supplied by Aladdin brand, photoinitiator 1173 was supplied by Shanghai yuanye Bio-Technology Co., Ltd., MAAR was supplied by Jiangsu Sanmu Group.

2.2 Synthesis of PGMA

The synthesis route of PGMA was based on previous work, shown in **Figure 2**. PGMA was prepared by phosphate acid and glycidyl methacrylate (GMA) (Chen and Jiao, 2008). Firstly, 10.8 g phosphate acid (0.11 mol) was added to the rounded bottom flask. Then 42.6 g GMA (0.3 mol) with 100 ml acetone was poured into the above solution dropwise in the condition of an ice bath. When the system is stable, the ice bath was removed and 1% methoxyphenol was added. Finally, the system was heated to 80°C and kept for 8 h. The water and acetone were removed by using rotary evaporators, thus obtaining the colorless product PGMA.

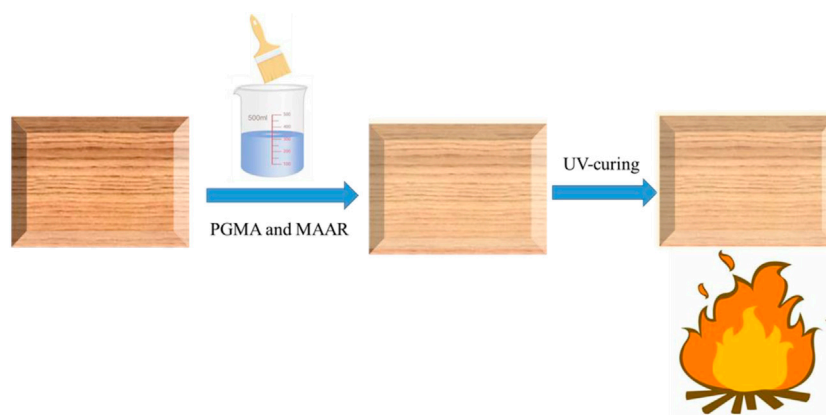
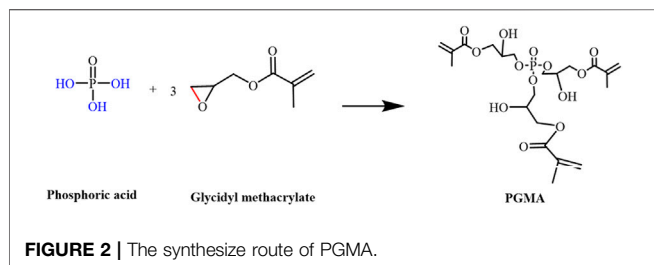


FIGURE 1 | Schematic of preparation of different coatings.

TABLE 1 | Formulation of different coatings.

Sample	PGMA (g)	MAAR (g)
Coating-1	10	0
Coating-2	6.67	3.33
Coating-3	5	5
Coating-4	3.33	6.67
Coating-5	0	10
Pure wood	0	0



2.3 UV-Curing Process of Different Coatings on Wood

The coatings of different ratios are shown in **Table 1**. The ultraviolet source is a UV curing machine with a power of 50 W.

First, PGMA and MAAR were blended at different proportions (1:0, 2:1, 1:1, 1:2, 0:1). 3 wt% photoinitiator (1173) was added into the mixture of all systems. Then, the wood was evenly brushed with these coatings. The samples of different proportions were cured under the exposure of ultraviolet rays. The thickness of coatings was controlled at the standard of 500 g/m².

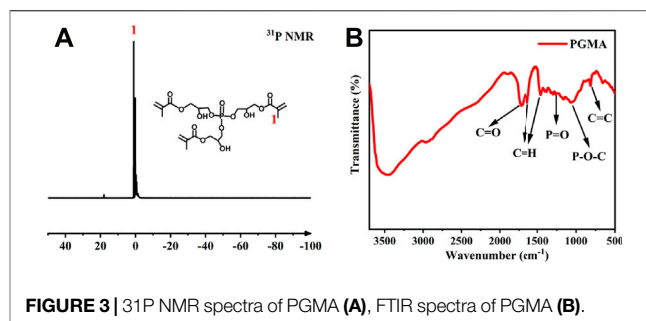
2.4 Characterization and Measurements

The structure of PGMA was characteristic by P31 NMR by an instrument of Avance 300 spectrometer (Bruker Biospin, Switzerland) with a solvent of CDCl₃.

Thermogravimetric analysis (TGA) was carried out to investigate the thermal stability of these coatings with a TGA Q5000 IR thermogravimetric analyzer (TA Instruments, New Castle, DE, United States) at a heating rate of 20°C min⁻¹.

The combustion behavior of coated wood was studied by cone calorimeter (FTT, Co., Ltd, Derby, United Kingdom) at a constant heat flux of 35 kW/m² at the standard of ISO 5660. The specimen of each sample was 100 mm × 100 mm × 3 mm.

In order to investigate the fire resistance of the different coatings on wood, the limiting oxygen index (LOI) was tested (The size of wood is 50 mm × 3 mm × 5 mm). An HC-2 type of oxygen index meter was carried out to test the LOI value of wood with different coatings. The test was carried out in the standard of ASTM D2863. In addition, we have designed a device to detect the change of back temperature on the uncoated side of wood when the coated side was on fire (The size of the wood was 100 mm × 100 mm × 3 mm). Butane was used as a source of fire. Thus, the



fire resistance of coated and uncoated wood could be easily compared by the two methods.

Scanning electron microscopy (SEM) was used to observe the morphology of char residue of coatings at an acceleration voltage of 10.0 kV.

Raman spectroscopy was performed by a SPEX-1403 laser Raman spectrometer (SPEX Co., United States) to test the degree of graphitization of the char layer.

X-ray photoelectron spectroscopy (XPS) is an effective way to detect the different element information of the surface of samples. Here, X-ray photoelectron spectroscopy (XPS) testing was performed with a VG ESCALB MK-II electron spectrometer.

Thermogravimetric analysis-infrared spectrometry (TG-IR) was tested from 20 to 700°C at 10°C min⁻¹ by a TGA Q5000IR thermogravimetric analyzer connected to a Nicolet 6700 FTIR spectrophotometer, with the N₂ atmosphere.

3 RESULT AND DISCUSSION

3.1 Synthesis and Characterization of PGMA

The structure and synthesis route are listed in **Figure 2**. The structure of PGMA was confirmed by ¹H NMR and ³¹P NMR spectra analysis. Previous reports have discussed the ¹H NMR

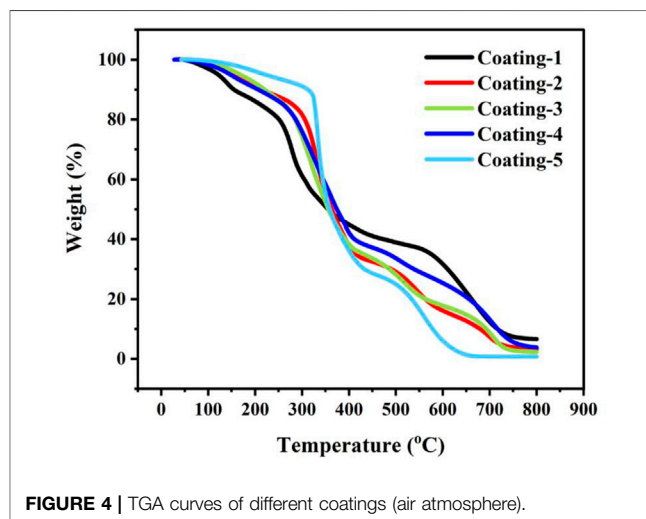


TABLE 2 | Cone calorimetry data.

Sample	pHRR (kW/m ²)	TTI (s)	THR (MJ/m ²)	TSR (m ² /m ²)
Coating-1	244.12	7	36.4	502.5
Coating-2	322.72	7	39.5	532.1
Coating-3	297.9237	9	36.5	477.2
Coating-4	238.83	3	38.4	512.4
Coating-5	414.74	8	44.6	449
Pure wood	249.29	4	39.0	622

spectra (Chen and Jiao, 2008). Hence, only the ³¹P NMR is shown here (Figure 3A).

FTIR spectra were carried out for better analyzing the structure of PGMA. As Figure 3B presented, the peaks at around 1726, 1636 and 1457 cm⁻¹ can correspond to the vibration of C=O and C=H bonds, respectively. The absorption peak that appeared at 3400 cm⁻¹ can be identified as the stretching vibration of H-O (Li et al., 2021a). The peaks located at 1068 cm⁻¹ and 1261 cm⁻¹ can be attributed to the vibration of P-O-C and P=O bonds, which confirm the formation of phosphonate. In addition, the characteristic peak of C=H can be observed in the wavenumber of 815 cm⁻¹ in FTIR spectra. Thus, PGMA was successfully fabricated as FTIR and ³¹P NMR spectra confirmed.

3.2 Thermal Stability of the Coatings

The thermal stability of UV-cured coatings was tested by a thermogravimetric analyzer. Air was chosen as the carrier gas for simulating the real process of pyrolysis. As shown in Figure 4, there are three decomposition stages of coating-1 which only contains PGMA. The first stage appearing near 200°C can be attributed to the degradation of the phosphate. With the temperature increasing, the second and third stages appeared at 328 and 367°C, corresponding to the thermal decomposition of the alkyl chain and the formation of poly (phosphoric acid), respectively. Besides, an extra weight loss maximum can be observed above 600°C, due to the decomposition of an unstable char layer. However, the initial thermal stability of UV-cured coatings increased with the addition of MAAR. As the TG curve of coating-5 shows, MAAR showed a rapid degradation process from 289°C and obtained a maximal weight loss at 347°C. There is no doubt that the UV-cured coatings which contain PGMA and MAAR at different proportions presented different thermal stability compared to coating-1 (PGMA) and coating-5 (MAAR). Moreover, coating-1 retained the higher mass residue of 11.74%, while the residue yield of coating-5 was only 2.428%. As a result, both the degradation process and char residue yield confirmed that the existence of PGMA is beneficial to the formation of a stable and protective char layer.

3.3 Cone Calorimeter Test

The cone calorimeter test was employed to explore the combustion behavior of coated and uncoated wood at a heat

flux of 35 kW/m². From the test, the heat release rate (HRR), total heat release (THR), CO production, CO₂ production, and total smoke release (TSR) results were obtained (Table 2).

3.3.1 Heat Release Rate

HRR is an effective way to measure the combustion behavior of materials (Zhou et al., 2020; Cai et al., 2021). The curves of the heat release rate are shown in Figure 5. As this figure revealed, there are two peaks in the HRR curves. The combustion of cellulose, hemicellulose, and lignin leads to a huge release of heat that forms the first exothermic peak. The second peak can be attributed to the combustion of molecules which was generated by the decomposition of cellulose, hemicellulose, and lignin. Obviously, the HRR value for the first stage of the coated wood has improved, probably due to the introduction of the PGMA (Zou et al., 2020). Previous research has already confirmed the existence of PGMA can produce phosphoric acid and polyphosphoric acid during pyrolysis, which can promote char formation to protect the substrates (Qu et al., 2020). With peak HRR value of the first stage improved faster and appeared earlier, the coating could be carbonized quicker. The quicker formed carbonization could prevent the inner structure of the wood from fire. Simultaneously, nonflammable gases such as NH₃, N₂, and NO₂ are released to dilute the O₂ in the air, which also results in a lower heat release. In detail, the peak HRR value of the second stage of wood with coating-4 is only 181.83 kW/m², which showed a 27.1% reduction compared to pure wood. The dramatic reduction suggests that the PGMA and MAAR probably have an excellent synergistic effect at a mass ratio of 1:2. In addition, the peak HRR in the second stage of coating-4 appeared later than other groups, and the HRR at the end of combustion was lower than other groups. The data of HRR reveals that coating-4 can significantly improve the fire resistance of wood.

3.3.2 Total Heat Release

The total heat release (THR) refers to the total amount of heat released during combustion. The curve of THR is shown in Figure 5B. The THR curves have a similar result as the HRR curves, showing that coating-4 performed best in the reduction of heat release. The wood with coating-1 and coating-2 showed a passive influence on total heat release. It can be concluded that a small amount of MAAR could not effectively reduce the concentration of O₂ or volatile organic compounds. The wood with coating-4 has the lowest THR value during the process of combustion. In addition, the wood with coating-4 burned for the longest time, indicating that coating-4 had well protected the wood substrate which can provide more time for escape.

3.3.3 Production of Carbon Monoxide and Carbon Dioxide

Both CO and CO₂ would be released in the combustion of wood and increase fire hazards (Hao et al., 2020). Therefore, it is significant to evaluate the CO and CO₂ release by cone calorimeter test. The CO and CO₂ curves are shown in

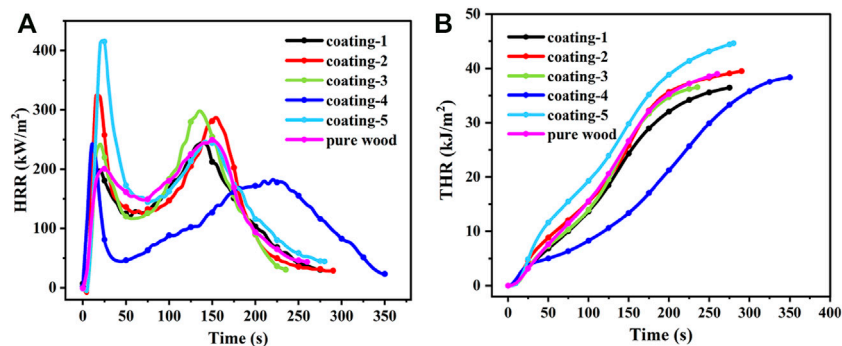


FIGURE 5 | The HRR (A) curves and THR (B) curves of the coated and pure wood.

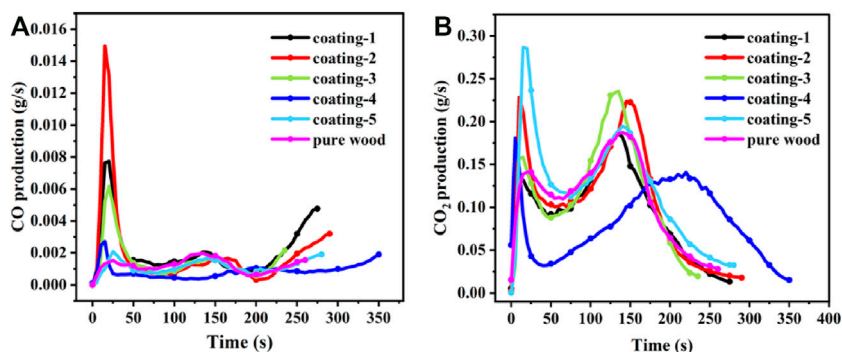


FIGURE 6 | CO₂ (A) and CO (B) production curves.

Figure 6. From the curves of CO₂ production, it is found the curves have the same trend as the HRR curves. Both the CO₂ production curves and the HRR curves include two stages due to the combustion of cellulose, hemicellulose, and lignin and the further combustion of small molecules. The wood with coating-4 showed the best effect on the delay and reduction of CO₂ production. However, the CO production curves are different. From **Figure 6**, the CO production of pure wood is much lower than the CO₂ production due to most of the CO can be transferred into CO₂ at a high heat flux (35 kW/m²). Compared with pure wood, the coated wood has an obvious peak in the CO production curves, which appears at 15 s after ignition. The production of CO was mainly attributed to the combustion of coatings. At the late time of combustion, the CO production was increased with the reduction of CO₂ production. The main reason is that the produced CO₂ reacts with the char layer to form CO. It is clear that the wood with coating-4 presented the lowest amount and longest time for CO production. As a result, the wood with coating-4 showed the lowest release of CO and CO₂ during combustion, suggesting better toxic gas suppression. There are two reasons for the wood with coating-4 causing the lowest CO and CO₂. Firstly, the dense char layer which is contributed by PGMA hindered the release of CO and CO₂. On the other hand, the releasing of vast nonflammable gases (NH₃, N₂, and NO₂) can significantly

slow the process of combustion leading to a lower release of CO and CO₂.

In addition, the coated wood boards exhibited a satisfying effect in improving the smoke suppression function during combustion. As **Table 2** shows, the TSR value of pure wood can reach 622 m²/m², while the TSR value of wood with coating-1, coating-2, coating-3, coating-4, and coating-5 decreased to 502.5, 532.1, 477.2, 512.4, and 449 m²/m², respectively. The dramatic reduction of TSR confirmed that these coatings can hinder the release of smoke, which can be attributed to the compact char layer caused by the combustion of coatings.

In conclusion, the wood with coating-4 showed the best result in the cone calorimeter test. The main reason is that PGMA and MAAR have the best synergistic effect in the proportion of coating-4. The PGMA would be decomposed to phosphorus acid to absorb a lot of heat and catalyze the char formation, while the MAAR could release nonflammable gases such as N₂, NH₃, or NO₂ that dilute the O₂ concentration. Thus, the compounded PGMA and MAAR showed a better effect on the reduction of heat release and smoke production.

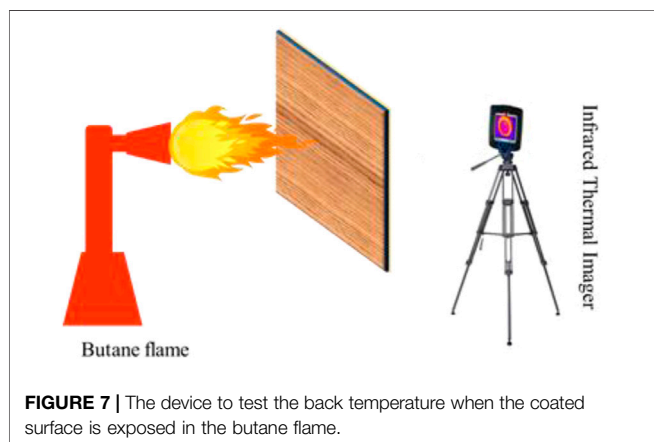
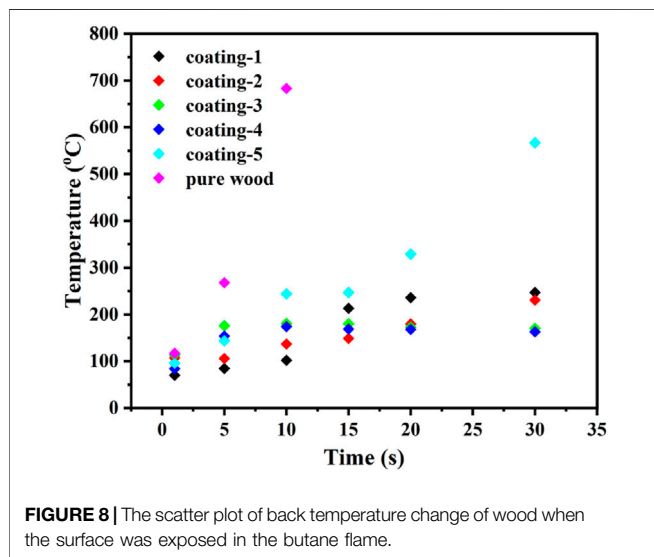
3.4 Fire Resistance Test of the Coated Wood

3.4.1 The Limiting Oxygen Index

The limiting oxygen index (LOI) test is an easy and directed way to test the fire resistance of different materials. The higher the LOI

TABLE 3 | LOI value of different coatings.

Samples	LOI value (%)
Coating-1	28
Coating-2	29
Coating-3	31
Coating-4	26
Coating-5	26
Pure wood	24

**FIGURE 7** | The device to test the back temperature when the coated surface is exposed in the butane flame.**FIGURE 8** | The scatter plot of back temperature change of wood when the surface was exposed in the butane flame.

value of the material is, the better the fire safety of the material. Here, the LOI values of six groups were obtained and shown in Table 3. From Table 3, it can be seen that the coating consisting of PGMA and MAAR has a positive effect on flame resistance. The LOI value of pure wood is only 24%. However, the LOI value of the wood with coating-3 is 31%. In addition, the LOI values of other groups also have been improved. These data proved that both the PGMA and MAAR could improve the fire resistance of wood. PGMA is a kind of phosphorus material, which can take an important role in the condensed phase flame retardancy effect.

Some works also proposed that the phosphorus materials could release PO or HPO radicals, which could combine with the H and HO radicals in the flame to put out a fire (Tang et al., 2018; Chi et al., 2020). MAAR is a kind of nitrogen-rich resin, which could generate lots of N_2 and NH_3 under fire. The vast nonflammable gases could dramatically decrease the density of flammable gases to slow down the fire. Therefore, both PGMA and MAAR are excellent flame retardants especially for their mixture in appropriate proportions.

3.4.2 Back Temperature Test

Another way to evaluate the fire resistance of the coated wood is to test the back temperature of wood when the coated surface is burning. The device and process are shown in Figure 7.

The infrared imager was used to record the change of back temperature. The images of back temperature at different times are shown in Figure 8.

From the test of back temperature, it can be seen that the existence of coating could significantly reduce the temperature of wood. The releasing of combustible gases and combustion heat were well restrained by these coatings, which led to improving the flame resistance of wood. The back temperature of pure wood has reached $700^{\circ}C$ when the surface was exposed to the flame for 10 minutes. However, the back temperatures of the coated woods were all below $250^{\circ}C$, which can be attributed to the barrier function of the coatings. The decomposition temperature of cellulose and hemicellulose are $180\text{--}340^{\circ}C$, while the pyrolysis temperature of lignin can reach up to $600^{\circ}C$. Thus, the fireproof coating could effectively prevent the lignin from combustion in the back temperature test. However, the back temperature of pure wood reached up to $700^{\circ}C$ after burning for 10 min, which can be attributed to the combustion of lignin. From the picture of wood before and after burning (Figure 9), it can be easily found that the coated woods maintained their structure better than the pure wood, and the char layer was more intumescent.

At the end of combustion, pure wood left less residuum. In addition, the back temperature of wood with coating-4 was only $163^{\circ}C$ after the coated wood had been exposed to flame for 30 min. This phenomenon suggested that coating-4 has a positive effect on improving the flame retardancy of wood.

3.5 Investigation on Char Residue

To better study the fire resistance mechanism of coated wood, the char residue of the coatings were tested with SEM, Raman spectroscopy, and X-ray photoelectron spectroscopy.

Scanning electron microscopy (SEM) was used to directly observe the morphology of the char layer. The char residue of coating-1, coating-4, and coating-5 was chosen to test. As Figure 10 presents, the char surfaces of the three samples are all compact and smooth, especially for the char layer of coating-4. These compact char layers suggested a favorable protection of inner materials when a fire occurs.

However, there is little distinction between each SEM figure. To further explore the properties of char residue, Raman spectra were carried out to test these samples. As Figure 11 reveals, the peaks that appeared at about 1360 and 1600cm^{-1} are corresponding to the D band and G band, respectively. The D

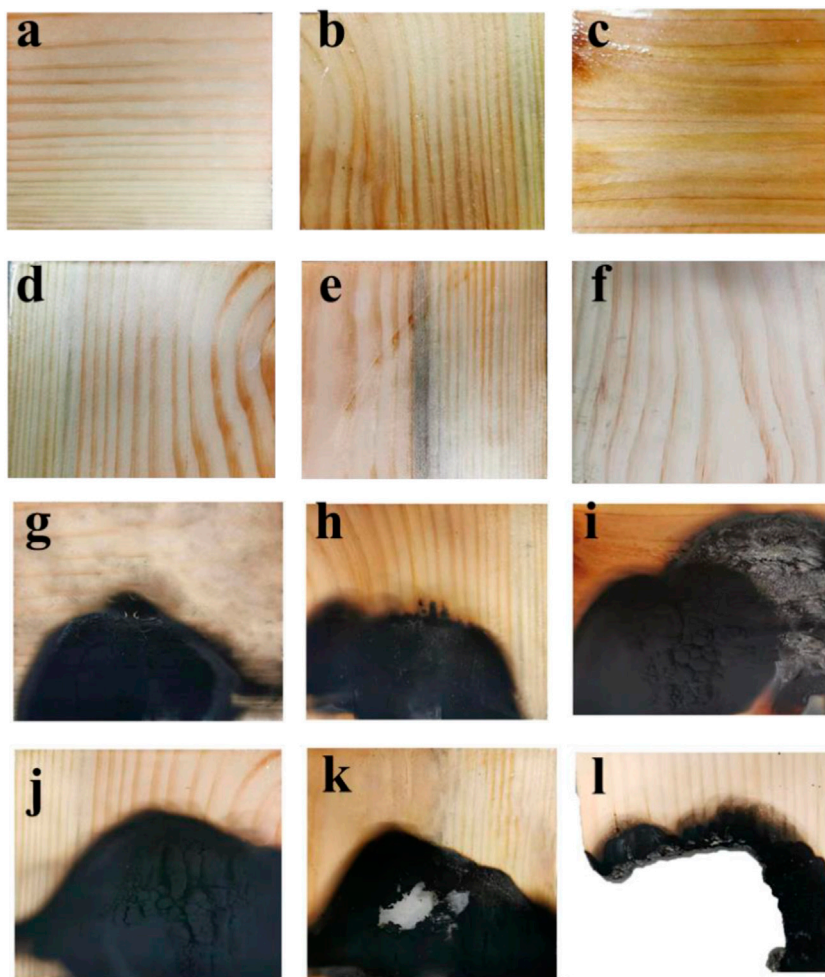


FIGURE 9 | Before back temperature test (A–F) and after back temperature test (G–L). (A–F), Wood with coating-1, coating-2, coating-3, coating-4, coating-5 and pure wood. (G–L), Wood with coating-1, coating-2, coating-3, coating-4, coating-5 and pure wood.)

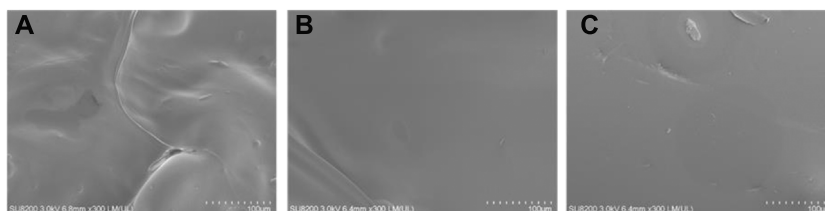


FIGURE 10 | SEM figures of char residue (A) coating-1 (B) coating-4 (C) coating-5.

band is related to the atomic lattice defect of C, while the appearance of the G band could be attributed to the sp^2 hybrid stretching vibration of C (Li et al., 2006). It is reliable to characterize the graphitization degree by comparing the intensity ratio of the G band to the D band (Li et al., 2021b). A higher graphitization degree suggested a better protection of materials from fire. The I_G/I_D values are 0.38, 0.96, and 0.32 corresponding to the char residue of coating-1, coating-4, and

coating-5, respectively. The value of I_G/I_D is proportional to the graphitization degree. The coating-4 has the highest graphitization degree after burning with an I_G/I_D value of 0.96, which means that coating-4 is capable of forming a more dense char layer to protect the inner materials.

X-ray photoelectron spectroscopy (XPS) was used to analyze the char residue of coating-1, coating-4, and coating-5 (Figure 12).

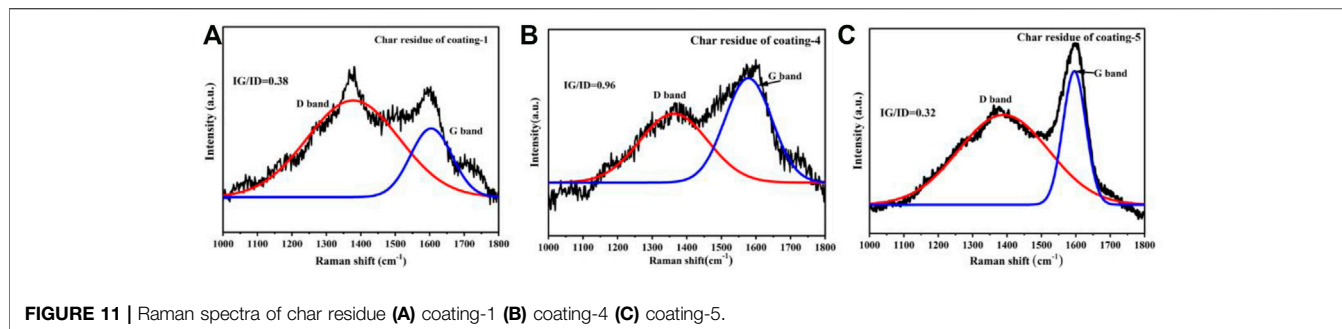


FIGURE 11 | Raman spectra of char residue (A) coating-1 (B) coating-4 (C) coating-5.

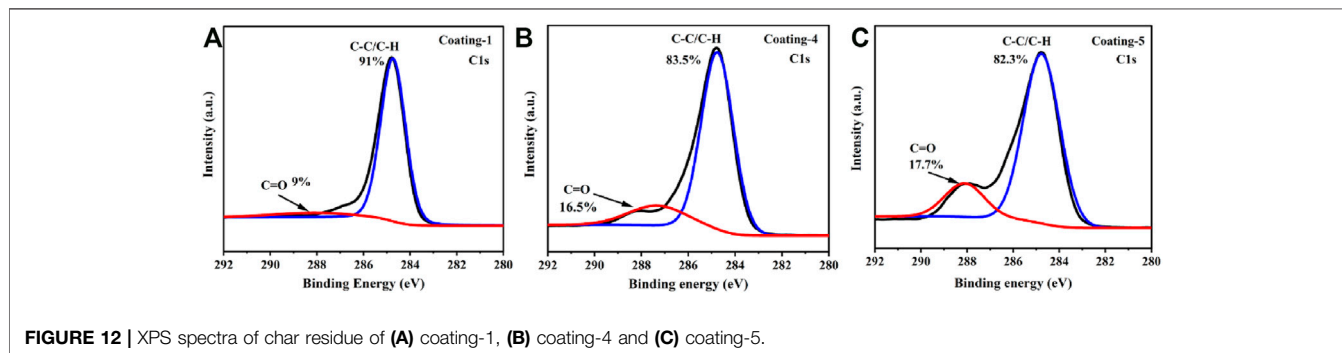


FIGURE 12 | XPS spectra of char residue of (A) coating-1, (B) coating-4 and (C) coating-5.

TABLE 4 | XPS results of char residues of different coatings.

Samples	Coating-1	Coating-4	Coating-5
C1s%	67.29	77.68	70.85
P2p%	5.77	0.95	0.09
N1s%	0.76	11.08	14.71
O1s%	26.18	10.29	14.34

Table 4 shows the XPS results of char residues of different coatings, from which the highest carbon content is presented in coating-4. In detail, char residue of coating-1 and coating-5 shows the value of C 1s at 67.29 and 70.85%, respectively, both of them are far below the value of coating-4 at 77.68%. A higher content of carbon indicates more carbon atoms were accumulated in char residue, demonstrating a better protective effect of coated materials. From XPS spectra of C1s, there are two peaks in binding energy at 284.8 and 288.7 eV, corresponding to C-C/C-H and C=O, respectively. It can be clearly seen that the peak intensity related to C-C/C-H of coating-1 is much higher than coating-4 and coating-5, suggesting that abundant C-C/C-H bonds existed in the cross-link structure of char residue. This phenomenon can be attributed to the high content of P element, which does well in forming a compact char layer during combustion. However, P-containing materials mainly act in the condensed phase of a fire which shows a limited effect on flame retardancy. Herein, the right amount of N-containing MAAR can improve the flame retardancy of coatings, due to MAAR mainly acting in

the gas phase by releasing vast nonflammable gases (Wang et al., 2018; Li et al., 2020). As a result, the coating showed the best fire resistance when the proportion of PGMA and MAAR is 1:2.

3.6 Pyrolysis Gas Analysis

To better study the flame retardant mechanism of the coatings, TG-FTIR analysis technology was exhibited to directly track and detect the gaseous small molecular compounds volatilized during the thermal degradation process. The curves from the TG-FTIR analysis of the coatings are shown in Figure 13. It can be inferred that different gases are produced as temp increased. The infrared characteristic peaks of the degradation product can be listed as 2960, 2340, 1760, and 1150 cm^{-1} , which could be attributed to the hydrocarbons, CO_2 , carbonyl, and ether, respectively (Liu et al., 2020). The infrared characteristic peak of CO_2 first appeared in Figure 13, probably due to the unstable P-O-C structure. As this figure reveals, the peak intensity of combustible volatiles such as C-H, C=O, and ethers are much lower in the degradation of coating-4, while the intensity of nonflammable gas (CO_2) peak is obviously higher. This phenomenon suggests that coating-4 has a positive effect on improving the fire resistance of wood. Phosphates (PGMA) decompose into polyphosphates at low temperatures and catalyze ethers to be transferred into the char layer and other small molecules. The ether of coating-1, which is composed of pure PGMA, shows the strongest intensity. For MAAR, the decomposed NH_3 , H_2O , and CO_2 are supposed to effectively dilute the combustible gases and simultaneously improve the intumescence of these coatings. In general, the

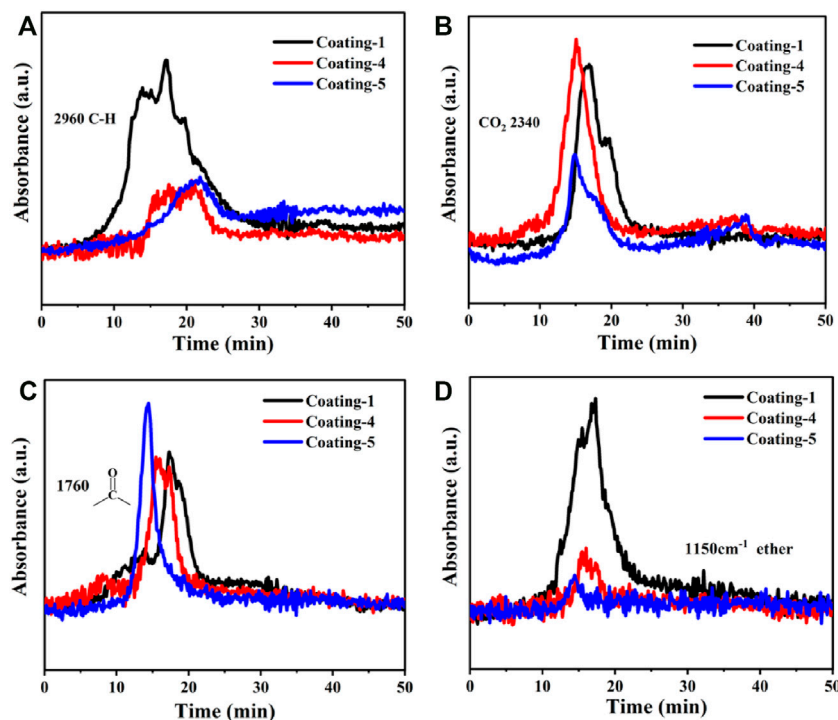


FIGURE 13 | TG-FTIR results of coating-1, 4 and 5. **(A)** C-H, **(B)** CO₂, **(C)** -C=O-, **(D)** ether.

coating consisting of PGMA and MAAR could act synergistically to prevent the wood substrate from fire hazards by forming a condensed char layer and diluting combustible gases with inert gases.

4 CONCLUSION

A series of transparent fire resistance coatings of wood consisting of PGMA and MAAR were fabricated successfully. The fire resistance of these coatings was investigated by cone calorimeter, back temperature, and LOI tests. The results showed that the wood with coating-4 (33.3% PGMA and 66.7% MAAR) had the best performance in the fire resistance. From the THR and HRR curves, the wood with coating-4 burned for the longest time indicating the PGMA and MAAR have the best synergistic effect in fire resistance. Specifically, PGMA acts in condensed phase to form a compact char layer for preventing the heat from transferring to inner materials in combustion, while MAAR could release vast nonflammable gases which showed a negative effect on fire at a suitable loading. To further investigate the flame retardant performance of coating-4, the SEM and Raman spectra were carried out to test the char residue of coating-4 and the results suggest a better protection of wood when compared with wood. Thus, the transparent coating consisting of PGMA and

MAAR provides a novel formula to fabricate effective fireproof of wood, which may promote the wider application of wood.

DATA AVAILABILITY STATEMENT

The original contributions presented in the study are included in the article/Supplementary Material, further inquiries can be directed to the corresponding authors.

AUTHOR CONTRIBUTIONS

The conception and design of the study: WX and YH Experiment and drafting the article: GM and XuW Analysis and interpretation of data: WC and CM Revising: YZ and XiW.

FUNDING

The research was financially supported by The National Key Research & Development (R&D) Plan of China under Grant No. 2020YFC1522800, Young Scientist Training Program of USTC (KY2320000018), USTC Tang Scholar, the National Key Research & Development (R&D) Plan of China under Grant No. 2020YFC1522800.

REFERENCES

- Cai, W., Li, Z., Mu, X., He, L., Zhou, X., Guo, W., et al. (2021). Barrier Function of Graphene for Suppressing the Smoke Toxicity of Polymer/black Phosphorous Nanocomposites with Mechanism Change. *J. Hazard. Mater.* 404, 124106. doi:10.1016/j.jhazmat.2020.124106
- Chen, X., and Jiao, C. (2008). Thermal Degradation Characteristics of a Novel Flame Retardant Coating Using TG-IR Technique. *Polym. Degrad. Stab.* 93, 2222–2225. doi:10.1016/j.polymdegradstab.2008.09.005
- Chi, Z., Guo, Z., Xu, Z., Zhang, M., Li, M., Shang, L., et al. (2020). A DOPO-Based Phosphorus-Nitrogen Flame Retardant Bio-Based Epoxy Resin from Diphenolic Acid: Synthesis, Flame-Retardant Behavior and Mechanism. *Polym. Degrad. Stab.* 176, 109151. doi:10.1016/j.polymdegradstab.2020.109151
- Guo, B., Liu, Y., Zhang, Q., Wang, F., Wang, Q., Liu, Y., et al. (2017). Efficient Flame-Retardant and Smoke-Suppression Properties of Mg-Al-Layered Double-Hydroxide Nanostructures on Wood Substrate. *ACS Appl. Mater. Inter.* 9, 23039–23047. doi:10.1021/acsami.7b06803
- Han, Y.-H., Taylor, A., Mantle, M. D., and Knowles, K. M. (2007). UV Curing of Organic-Inorganic Hybrid Coating Materials. *J. Sol-gel Sci. Technol.* 43, 111–123. doi:10.1007/s10971-007-1544-8
- Hao, H., Chow, C. L., and Lau, D. (2020). Effect of Heat Flux on Combustion of Different wood Species. *Fuel* 278, 118325. doi:10.1016/j.fuel.2020.118325
- Jiang, J., Li, J., and Gao, Q. (2015). Effect of Flame Retardant Treatment on Dimensional Stability and thermal Degradation of wood. *Constr. Build. Mater.* 75, 74–81. doi:10.1016/j.conbuildmat.2014.10.037
- Li, L., Liu, X., Shao, X., Jiang, L., Huang, K., and Zhao, S. (2020). Synergistic Effects of a Highly Effective Intumescent Flame Retardant Based on Tannic Acid Functionalized Graphene on the Flame Retardancy and Smoke Suppression Properties of Natural Rubber. *Compos. A: Appl. Sci. Manuf.* 129, 105715. doi:10.1016/j.compositesa.2019.105715
- Li, X., Hayashi, J., and Li, C. (2006). FT-Raman Spectroscopic Study of the Evolution of Char Structure during the Pyrolysis of a Victorian Brown Coal. *Fuel* 85, 1700–1707. doi:10.1016/j.fuel.2006.03.008
- Li, Z., Lei, S., Xi, J., Ye, D., Hu, W., Song, L., et al. (2021a). Bio-based Multifunctional Carbon Aerogels from Sugarcane Residue for Organic Solvents Adsorption and solar-thermal-driven Oil Removal. *Chem. Eng. J.* 426, 129580. doi:10.1016/j.cej.2021.129580
- Li, Z., Zhu, Y., Xi, J., Ye, D., Hu, W., Song, L., et al. (2021b). Scalable Production of Hydrophobic and Photo-thermal Conversion Bio-Based 3D Scaffold: Towards Oil-Water Separation and Continuous Oil Collection. *J. Clean. Prod.* 319, 128567. doi:10.1016/j.jclepro.2021.128567
- Liu, Y., Xu, B., Qian, L., Chen, Y., and Qiu, Y. (2020). Impact on Flame Retardancy and Degradation Behavior of Intumescent Flame-retardant EP Composites by a Hyperbranched Triazine-based Charring Agent. *Polym. Adv. Technol.* 31, 3316–3327. doi:10.1002/pat.5055
- Lu, J., Jiang, P., Chen, Z., Li, L., and Huang, Y. (2021). Flame Retardancy, thermal Stability, and Hygroscopicity of wood Materials Modified with Melamine and Amino Trimethylene Phosphonic Acid. *Constr. Build. Mater.* 267, 121042. doi:10.1016/j.conbuildmat.2020.121042
- Ma, T., Li, L., Liu, Z., Zhang, J., Guo, C., and Wang, Q. (2020). A Facile Strategy to Construct Vegetable Oil-Based, Fire-Retardant, Transparent and Mussel Adhesive Intumescent Coating for wood Substrates. *Ind. Crops Prod.* 154, 112628. doi:10.1016/j.indcrop.2020.112628
- Ma, T., Li, L., Wang, Q., and Guo, C. (2019). Construction of Intumescent Flame Retardant and Hydrophobic Coating on wood Substrates Based on Thiol-Ene Click Chemistry without Photoinitiators. *Compos. B: Eng.* 177, 107357. doi:10.1016/j.compositesb.2019.107357
- Pabellina, K. G., Lumban, C. O., and Ramos, H. J. (2012). Plasma Impregnation of wood with Fire Retardants. *Nucl. Instr. Methods Phys. Res. Sect. B: Beam Interact. Mater. Atoms* 272, 365–369. doi:10.1016/j.nimb.2011.01.102
- Qu, Z., Wu, K., Jiao, E., Chen, W., Hu, Z., Xu, C., et al. (2020). Surface Functionalization of Few-Layer Black Phosphorene and its Flame Retardancy in Epoxy Resin. *Chem. Eng. J.* 382, 122991. doi:10.1016/j.cej.2019.122991
- Song, K., Ganguly, I., Eastin, I., and Dichiaro, A. (2020). High Temperature and Fire Behavior of Hydrothermally Modified wood Impregnated with Carbon Nanomaterials. *J. Hazard. Mater.* 384, 121283. doi:10.1016/j.jhazmat.2019.121283
- Tang, S., Qian, L., Qiu, Y., and Dong, Y. (2018). Synergistic Flame-Retardant Effect and Mechanisms of boron/phosphorus Compounds on Epoxy Resins. *Polym. Adv. Technol.* 29, 641–648. doi:10.1002/pat.4174
- Wang, T., Liu, T., Ma, T., Li, L., Wang, Q., and Guo, C. (2018). Study on Degradation of Phosphorus and Nitrogen Composite UV-Cured Flame Retardant Coating on wood Surface. *Prog. Org. Coat.* 124, 240–248. doi:10.1016/j.porgcoat.2018.08.017
- Xu, J., Jiang, Y., Zhang, T., Dai, Y., Yang, D., Qiu, F., et al. (2018). Synthesis of UV-Curing Waterborne Polyurethane-Acrylate Coating and its Photopolymerization Kinetics Using FT-IR and Photo-DSC Methods. *Prog. Org. Coat.* 122, 10–18. doi:10.1016/j.porgcoat.2018.05.008
- Yan, L., Xu, Z., and Liu, D. (2019). Synthesis and Application of Novel Magnesium Phosphate Ester Flame Retardants for Transparent Intumescent Fire-Retardant Coatings Applied on wood Substrates. *Prog. Org. Coat.* 129, 327–337. doi:10.1016/j.porgcoat.2019.01.013
- Yan, L., Xu, Z., and Wang, X. (2018). Synergistic Flame-Retardant and Smoke Suppression Effects of Zinc Borate in Transparent Intumescent Fire-Retardant Coatings Applied on wood Substrates. *J. Therm. Anal. Calorim.* 136, 1563–1574. doi:10.1007/s10973-018-7819-1
- Yan, X., Qian, X., Lu, R., and Miyakoshi, T. (2017). Synergistic Effect of Addition of Fillers on Properties of Interior Waterborne UV-Curing Wood Coatings. *Coatings* 8, 9. doi:10.3390/coatings8010009
- Zhou, F., Zhang, T., Zou, B., Hu, W., Wang, B., Zhan, J., et al. (2020). Synthesis of a Novel Liquid Phosphorus-Containing Flame Retardant for Flexible Polyurethane Foam: Combustion Behaviors and thermal Properties. *Polym. Degrad. Stab.* 171, 109029. doi:10.1016/j.polymdegradstab.2019.109029
- Zou, B., Qiu, S., Ren, X., Zhou, Y., Zhou, F., Xu, Z., et al. (2020). Combination of Black Phosphorus Nanosheets and MCNTs via Phosphorus Carbon Bonds for Reducing the Flammability of Air Stable Epoxy Resin Nanocomposites. *J. Hazard. Mater.* 383, 121069. doi:10.1016/j.jhazmat.2019.121069

Conflict of Interest: Author GM is employed by Beijing Building Materials Testing Academy Co., Ltd. National Center for Safety Quality Supervision and Testing of Fire-proof Building Products.

The remaining authors declare that the research was conducted in the absence of any commercial or financial relationships that could be construed as a potential conflict of interest.

Publisher's Note: All claims expressed in this article are solely those of the authors and do not necessarily represent those of their affiliated organizations, or those of the publisher, the editors and the reviewers. Any product that may be evaluated in this article, or claim that may be made by its manufacturer, is not guaranteed or endorsed by the publisher.

Copyright © 2022 Ma, Wang, Cai, Ma, Wang, Zhu, Kan, Xing and Hu. This is an open-access article distributed under the terms of the Creative Commons Attribution License (CC BY). The use, distribution or reproduction in other forums is permitted, provided the original author(s) and the copyright owner(s) are credited and that the original publication in this journal is cited, in accordance with accepted academic practice. No use, distribution or reproduction is permitted which does not comply with these terms.